

On the quadruple Beltrami fields in thermally relativistic electron-positron-ion plasma

Usman Shazad* and M Iqbal

*Department of Physics, University of Engineering and Technology, Lahore 54890, Pakistan**

A thermally relativistic electron-positron-ion (EPI) plasma self-organizes into a quadruple Beltrami (QB) field. The QB field, which is the combination of four Beltrami fields, is described by four scale parameters. These scale parameters are often either real or both real and complex in nature. The values of the scale parameters are determined by Beltrami parameters, relativistic temperatures, and the densities of plasma species. It is demonstrated that all the scale parameters become real at higher relativistic temperatures and ion densities, which naturally lead to paramagnetic structures. It is also shown that the scale separation in the QB state provides the possibility of field and flow generation in such thermally relativistic plasmas. The present study may have implications for space, astrophysical and laboratory plasmas.

I. INTRODUCTION

Magnetic self-organization, commonly referred to as plasma relaxation, is the process of minimizing plasma energy under helicity constraints. The Beltrami fields are typically used to characterize these relaxed states. A Beltrami field is an eigenvector of the curl operator. For instance, when the magnetic energy of an ideal MHD plasma under magnetic helicity constraint is minimized, the relaxed state is a single Beltrami state, which is expressed as $\nabla \times \mathbf{B} = \mu \mathbf{B}$, where μ is constant and eigenvalue of the curl operator. In the single Beltrami state, the current density is aligned to the magnetic field, so the relaxed state is force-free and flow-less [1–3].

Plasmas in nature or a laboratory aren't force-free and flow-less, hence the single fluid

*Electronic address: usmangondle@gmail.com

MHD theory was extended to account for novel relaxed states with significant plasma flow and pressure gradients. Multifluid plasma self-organization models suggest a non-force-free relaxed state. The self-organized state of multifluid plasmas can be described as a combination of multiple Beltrami fields. For example, the relaxed state in Hall MHD represents the combination of two Beltrami fields, which is referred to as a double Beltrami (DB) state [4–6]. On the other hand, the inclusion of inertial effects results in a relaxed state that is composed of three Beltrami fields and is referred to as a triple Beltrami (TB) state. In comparison to MHD relaxation, relaxed multifluid plasmas have substantial flow and pressure gradients. When compared to single fluid MHD relaxation, which has only one macroscopic scale, the self-organized state of two or multicomponent plasmas is characterized by multi-scale structures (both macroscopic and microscopic structures) [7–11]. The multi-Beltrami relaxed states in plasmas allow for the formation of very novel and complex structures, which are applied to the study of a wide range of physical phenomena that occur in the laboratory and in space. For instance, high beta relaxed states in tokamak [12–14], formation and heating of solar corona [15, 16], eruptive events in space plasma [17, 18], acceleration of plasma flows [19], dynamo/reverse dynamo mechanisms [20, 21], turbulence [22, 23] and etc.

The goal of this study is to explore the relaxed states of a thermally relativistic electron, positron and ion (EPI) plasma. The EPI plasmas can be found in a number of different astrophysical environments and can also be created in a laboratory. These astrophysical environments include the early universe [24], pulsar magnetospheres [25–29], accretion disks around black holes [30], active galactic nuclei (AGN) [31], gamma-ray bursts [32], supernova remnants [33] and solar flares [34]. In the laboratory it is also possible to produce EPI plasmas by injecting positrons into the electron ion system and through ultra-intense laser matter interactions [35–40]. The EPI plasmas in these astrophysical objects and laboratory experiments are usually in the relativistic regime. Plasma is relativistic when its fluid velocity approaches the speed of light or when its average kinetic energy surpasses its rest mass energy.

In recent years, many researchers have studied self-organization in relativistic plasmas. A study by Iqbal et al. has shown that the relaxed state of a relativistically hot EP plasma is a TB state. It has been demonstrated that at higher thermal energy, all of the scale parameters are real, and the size of one of the structures grows larger with an increase in the amount of thermal energy [41]. The relaxed state is likewise a TB state when all

of the inertial effects of a relativistically hot three-component EPI plasma are taken into consideration. It has been shown that a rise in relativistic temperature affects one self-organized structure more than the other two structures. At higher relativistic temperatures, two separate structures eventually become a single one. This demonstrates that diamagnetic plasma structures in such relativistic hot plasmas are possible [42, 43]. In another study, the variational approach was used to obtain a relaxed state for a fully relativistic plasma (one in which the fluid velocity as well as the thermal energy are both relativistic). This state was used to replicate the striped wind phenomena that occur in the pulsar nebula [44]. For a relativistically hot EPI plasma that contains static ions, the self-organized state is also a TB state. The parametric study of the relaxed state reveals that when the thermal energy and ion density increase, the scale separation grows, and the diamagnetic structures eventually transform into the paramagnetic structures [45].

In the past few years, the field of plasma relaxation has been extended to include relativistic degenerate plasmas. It has been investigated that a Beltrami-Bernoulli equilibrium state with electron degeneracy pressure is also possible. Even in a zero-temperature plasma, a Beltrami-Bernoulli equilibrium state can be obtained due to electron degeneracy. These states are being investigated in order to better depict new pathways for the transformation of energy, such as the conversion of degeneracy energy to fluid kinetic energy [46]. Shatashvili et al. have further explored the relaxed states of such relativistic degenerate plasmas to understand the impact of relativistic degeneracy on the multiscale relaxed state structures. It has been studied that a three-component plasma with relativistic degenerate electrons and positrons and mobile classical ions is a quadruple Beltrami (QB) state. In the same way, a QB state can also be reached with a three-component plasma made up of mobile classical ions and electrons with two temperatures (relativistic degenerate and classical hot). The investigation of these QB states has shed light on the role that degeneracy-induced relativistic temperature has on the formation of multiscale structures [47, 48]. Plasma relaxation is also the focus of a great deal of research that takes into consideration the implications of general relativity as such relativistic plasmas are also encountered in the vicinity of black holes [49–52].

In the present study which is extension of our previous work [45], we consider a three-component thermally relativistic EPI plasma. In a thermally relativistic plasma, the thermal energy of plasma species is on the order of or greater than their rest mass energy, whereas the

fluid velocity of the plasma species is considered to be non-relativistic. In recent years, a lot of research has been done on such EPI plasmas with thermal relativistic effects [53–58]. In our plasma model, the relativistic temperatures of electrons and positrons are assumed to be equal, whereas the relativistic temperature of ions is taken differently and considered mildly relativistic. Such thermally relativistic two-temperature plasmas with sub-relativistic ions are created in low density and high temperature astrophysical systems due to relativistic radiative turbulence. The some examples of such astrophysical systems are hot accretion flows, the galactic center, M87 and pulsar magnetospheres [59, 60]. It is shown that the relaxed state is the QB state. The effect of plasma parameters on the relaxed state has been investigated. For given values of the Beltrami parameters, the density and thermal energy of pair species have been demonstrated to be able to convert diamagnetic structures into paramagnetic ones and vice versa. The study also highlights the impact of scale separation in QB state in the context of dynamo and reverse dynamo mechanisms.

The structure of the paper is as follows: The model equations and the QB relaxed state equation is derived in Sec. II. The characteristics of the scale parameters are discussed in Sec. III. The following section provides an analytical solution for the QB field and flow in simple slab geometry and investigates the impact of plasma parameters and scale separation on relaxed state structures. The summary of the current study can be found in Sec. V.

II. MODEL EQUATIONS AND QB FIELDS

In this study, we consider a three-component incompressible, collisionless, quasi-neutral and magnetized plasma whose components are electrons, positrons and ions (in model equations we will use α for plasma species, e –electron, p –positron and i –ion). All of the plasma species are dynamic and only thermally relativistic. A plasma is said to be relativistic when the directed fluid velocity approaches the speed of light or the thermal energy of plasma particles is the order of or equal to the rest mass energy. Both approaches to relativity emerge in astrophysical and laboratory plasmas. By following Ref. [61], if the velocity distribution of α plasma species is local relativistic Maxwellian, the relativistic equation of motion can be expressed as:

$$\frac{\partial \mathbf{P}_\alpha}{\partial t} + m_{o\alpha} c^2 \nabla (\gamma_\alpha G_\alpha) = q_\alpha \mathbf{E} + \mathbf{V}_\alpha \times \left(\mathbf{P}_\alpha + \frac{q_\alpha}{c} \mathbf{B} \right), \quad (1)$$

where $\mathbf{P}_\alpha = \gamma_\alpha G_\alpha m_{0\alpha} \mathbf{V}_\alpha$, c , \mathbf{V}_α , γ_α , G_α , $m_{0\alpha}$ and q_α are relativistic momentum, speed of light, plasma velocity, Lorentz factor ($1/\sqrt{1 - V_\alpha^2/c^2}$), relativistic temperature, rest mass and electric charge respectively. The \mathbf{E} and \mathbf{B} are electric and magnetic fields which are related to scalar electric potential ϕ and vector magnetic potential \mathbf{A} by the following relations: $\mathbf{E} = -\nabla\phi - c^{-1}\partial\mathbf{A}/\partial t$ and $\mathbf{B} = \nabla \times \mathbf{A}$. In above equation the streaming relativistic effects accounted through γ_α while the thermal relativistic effects appear through the factor $G_\alpha = K_3(1/z_\alpha)/K_2(1/z_\alpha)$, where K_2 and K_3 are the modified Bessel functions and $z_\alpha = T_\alpha/m_{0\alpha}c^2$, where T_α is proper temperature of the plasma species. For non-relativistic case $z_\alpha \ll 1$, and the factor G_α can approximately be taken as $G_\alpha \simeq 1 + 5z_\alpha/2$, whereas for highly relativistic plasma species $z_\alpha \gg 1$ and the relativistic temperature G_α can be approximated as $G_\alpha \simeq 4z_\alpha$. It is essential to point out that the preceding equation of motion is supplemented with the following equation of state:

$$\frac{n_\alpha}{\gamma_\alpha} \frac{z_\alpha}{K_2(z_\alpha)} \exp(-z_\alpha G_\alpha) = \text{constant}. \quad (2)$$

Following Shatashvili et al. [47], we'll start with macroscopic evolution equations for multi-fluid relativistic hot plasma to derive the QB state. The curl of these equations will yield vorticity evolution equations. The steady state solution of these vorticity evolution equations provides three Beltrami conditions. The Beltrami conditions basically show the alignment of generalized vorticity with the respective flow. To couple the steady state dynamics of plasma species given by the Beltrami condition, we will employ Ampere's law. By solving these three Beltrami conditions along with Ampere's law, we will obtain a QB relaxed state equation.

Since we will only be considering plasma that is thermally relativistic, the flow velocity of plasma species will be non-relativistic and hence $\gamma_\alpha \approx 1$. Furthermore, we assume that electrons and positrons have the same relativistic temperature ($G_e = G_p = G$) whereas ions have a different relativistic temperature (G_i). The quasi-neutrality condition for the plasma system is $N_i + N_p = 1$, where N_i and N_p are n_{0i}/n_{0e} and n_{0p}/n_{0e} respectively, in which n_{0e} , n_{0p} and n_{0i} are the number densities of electron, positron and ion species in rest frame of reference. The macroscopic evolution equations of thermally relativistic two temperature EPI plasma in normalized form (for normalization of length, plasma species velocity, temperature and magnetic field we have used electron skin depth $\lambda_e = \sqrt{m_{0e}c^2/4\pi n_{0e}e^2}$, Alfvén speed $v_A = B_0/\sqrt{4\pi m_{0e}n_{0e}}$, electron plasma frequency $\omega_{pe} = \sqrt{4\pi n_{0e}e^2/m_{0e}}$, rest mass en-

ergy of electron $m_{0e}c^2$ and some arbitrary value of magnetic field B_0 , respectively) can be expressed as

$$\frac{\partial \mathbf{P}_\alpha}{\partial t} = \mathbf{V}_\alpha \times \boldsymbol{\Omega}_\alpha - \nabla \psi_\alpha, \quad (3)$$

where $\mathbf{P}_e = G\mathbf{V}_e - \mathbf{A}$, $\mathbf{P}_p = G\mathbf{V}_p + \mathbf{A}$, $\mathbf{P}_i = G_i\mathbf{V}_i + M\mathbf{A}$, $\boldsymbol{\Omega}_e = \nabla \times \mathbf{P}_e$, $\boldsymbol{\Omega}_p = \nabla \times \mathbf{P}_p$, $\boldsymbol{\Omega}_i = \nabla \times \mathbf{P}_i$, $\psi_e = -\phi - G$, $\psi_p = \phi - G$ and $\psi_i = M\phi - G_i$ and $M = m_{0e}/m_{0i}$ in which m_{0e} and m_{0i} are rest masses of electron and ion. In above equations of motion \mathbf{P}_α and $\boldsymbol{\Omega}_\alpha$ are termed as canonical/generalized momentum and vorticity respectively. To couple the dynamics of plasma species and close the system of equations, Ampere's law is adopted. For this plasma system, Ampere's law in dimensionless form is

$$\nabla \times \mathbf{B} = N_p \mathbf{V}_p + N_i \mathbf{V}_i - \mathbf{V}_e. \quad (4)$$

To obtain the vorticity evolution equations we take curl of the momentum equations (3), the following vorticity evolution equations are obtained

$$\frac{\partial \boldsymbol{\Omega}_\alpha}{\partial t} = \nabla \times [\mathbf{V}_\alpha \times \boldsymbol{\Omega}_\alpha]. \quad (5)$$

The steady-state solution of equation (5) with the condition $\mathbf{V}_\alpha \times \boldsymbol{\Omega}_\alpha = 0$, defines the multi-Beltrami equilibrium state provided that the gradient forces $\nabla \psi_\alpha$ are separately constrained to zero. The latter provides the generalized Bernoulli conditions, which are necessary for closure, although they are not important for the analysis described in this article. This solution yields three Beltrami conditions ($\mathbf{V}_\alpha \parallel \boldsymbol{\Omega}_\alpha$) for electrons, positrons and ions. These Beltrami conditions are given by

$$\nabla \times G\mathbf{V}_e - \mathbf{B} = aG\mathbf{V}_e, \quad (6)$$

$$\nabla \times G\mathbf{V}_p + \mathbf{B} = bG\mathbf{V}_p, \quad (7)$$

$$\nabla \times G_i\mathbf{V}_i + M\mathbf{B} = cG_i\mathbf{V}_i, \quad (8)$$

where a , b and c are the Beltrami parameters. The Beltrami parameters are ratios of generalized vorticities to their respective flows. The equations (4 and 6-8) will be employed to derive a relaxed state. By solving these equations simultaneously, the expression for ion species velocity \mathbf{V}_i in terms of magnetic field can be expressed as

$$\mathbf{V}_i = i_4(\nabla \times)^3 \mathbf{B} - i_3(\nabla \times)^2 \mathbf{B} + i_2 \nabla \times \mathbf{B} - i_1 \mathbf{B}, \quad (9)$$

where $i_4 = \alpha_3^{-1}$, $i_3 = (a+b)\alpha_3^{-1}$, $i_2 = (ab+\alpha_1)\alpha_3^{-1}$, $i_1 = (\alpha_2+\alpha_1b)\alpha_3^{-1}$, $\alpha_1 = (1+N_p)G^{-1}+MN_iG_i^{-1}$, $\alpha_2 = N_p(a-b)G^{-1}+MN_i(a-c)G_i^{-1}$ and $\alpha_3 = N_i(a-c)(b-c)$. Similarly the expression for \mathbf{V}_p in terms of \mathbf{B} can be written as

$$\mathbf{V}_p = p_4(\nabla \times)^3 \mathbf{B} - p_3(\nabla \times)^2 \mathbf{B} + p_2 \nabla \times \mathbf{B} - p_1 \mathbf{B}, \quad (10)$$

where $p_4 = i_4 N_i p(a-c)$, $p_3 = i_3 N_i p(a-c) - p$, $p_2 = i_2 N_i p(a-c) - ap$, $p_1 = b_1 N_i p(a-c) - \alpha_1 p$ and $p = N_p^{-1}(b-a)^{-1}$. By substituting the values of \mathbf{V}_i , \mathbf{V}_p from equations (9-10) into equation (4), the expression for \mathbf{V}_e is

$$\mathbf{V}_e = e_4(\nabla \times)^3 \mathbf{B} - e_3(\nabla \times)^2 \mathbf{B} + e_2 \nabla \times \mathbf{B} - e_1 \mathbf{B}, \quad (11)$$

where $e_4 = N_p p_4 + N_i i_4$, $e_3 = N_p p_3 + N_i i_3$, $e_2 = N_p p_2 + N_i i_2 - 1$ and $e_1 = N_p p_1 + N_i i_1$. To view the behavior of composite flow of plasma in relaxed state we find the relation for composite velocity \mathbf{V} given by

$$\mathbf{V} = \frac{M\mathbf{V}_e + MN_p\mathbf{V}_p + N_i\mathbf{V}_i}{M + MN_p + N_i}. \quad (12)$$

By plugging in the values of \mathbf{V}_i , \mathbf{V}_p and \mathbf{V}_e from equations (9-11) in above relation, the relation for \mathbf{V} becomes

$$\mathbf{V} = f_4(\nabla \times)^3 \mathbf{B} - f_3(\nabla \times)^2 \mathbf{B} + f_2 \nabla \times \mathbf{B} - f_1 \mathbf{B}, \quad (13)$$

where $f_{j=1,2,3,4} = f(N_i i_j + MN_p p_j + M e_j)$ and $f = (M + MN_p + N_i)^{-1}$. To obtain a relaxed state equation for magnetic field, we substitute the value of \mathbf{V}_i from equation (9) in equation (8) which leads to the following equation

$$(\nabla \times)^4 \mathbf{B} - k_4(\nabla \times)^3 \mathbf{B} + k_3(\nabla \times)^2 \mathbf{B} - k_2 \nabla \times \mathbf{B} + k_1 \mathbf{B} = 0, \quad (14)$$

where $k_4 = a+b+c$, $k_3 = ab+ac+bc+G^{-1}(1+N_p+G_i^{-1}MN_i)$, $k_2 = G^{-1}(b+c+aN_p+cN_p)+abc+G_i^{-1}MN_i(a+b)$ and $k_1 = cG^{-1}(b+aN_p)+abG_i^{-1}MN_i$. The relaxed state equation (14), is QB equation which can be expressed as superposition of four single Beltrami fields. The QB state in thermally relativistic two temperature EPI plasma is the consequence of taking into account inertia of all the plasma species and three distinct Beltrami parameters for each plasma species. It is also very important to note that the expressions for plasma species velocities and composite velocity show strong magnetofluid coupling and all the vector fields (\mathbf{V}_e , \mathbf{V}_p , \mathbf{V}_i and \mathbf{B}) are QB fields for this plasma model.

In this plasma model lower index Beltrami states (DB and TB) can also be obtained by adjusting the Beltrami parameters. For instance, a TB relaxed state emerges when the ratios of generalized vorticity to the flow of any two plasma species are equal to one another (have the same values of Beltrami parameters) [43]. Similar is the case when the flow vorticity of any two plasma species is aligned to magnetic field, the relaxed state comes out to be TB state. If the flows of plasma species are adjusted in such a way that the ratios of generalized vorticities to flows become equal for all of the plasma species, one can obtain a DB state.

In 2008, Mahajan demonstrated theoretically that a perfect diamagnetic state is also possible in a magnetized classical plasma. To achieve this diamagnetic relaxed state, which he termed as "classical perfect diamagnetism (CPD)" in classical single-fluid plasma, flow vorticity was aligned with the magnetic field. He also proposed that by experimenting with different methods of injecting particle beams into the ambient plasma, it is possible to create an infinitesimally small helicity of plasma species [62]. In order to get a glimpse of CPD in thermally relativistic EPI, we assume that the flow vorticities of all the plasma species become parallel to the magnetic field. This is a special class of steady state solution to the vorticity evolution equations. The vanishing of generalized helicity of all the plasma species is the singular limit for this plasma system, which is only feasible when electromagnetic, kinematic and thermal forces are all in balance. So from equations (4 and 6-8), under above assumption we obtain the following equation for CPD

$$\nabla \times \nabla \times \mathbf{B} + k\mathbf{B} = 0, \quad (15)$$

where $k = G^{-1}(1 + N_p) + MN_i G_i^{-1}$. It is also clear from equation (15) that relativistic temperatures and plasma species densities can also influence the strength of diamagnetism in the relaxed state. More recently, Asenjo and Mahajan studied similar perfect diamagnetic states in a cosmic plasma consisting of electrons and positrons in the radiation epoch of the early universe. They proposed that for the expanding cosmological plasmas in a curved space-time, the electromagnetic, kinematic, and thermal forces can come to balance, resulting in the disappearance of the generalized helicities of plasma species, and as a result, there is a diamagnetic trend in the magnetic field [51].

III. CHARACTERISTICS OF SCALE PARAMETERS

The commutative nature of curl operator dictate us that the QB equation (14) can also be written as

$$(\text{curl} - \mu_1)(\text{curl} - \mu_2)(\text{curl} - \mu_3)(\text{curl} - \mu_4)\mathbf{B} = 0,$$

where μ_1 , μ_2 , μ_3 , and μ_4 are the eigenvalues of the curl operator and also called scale parameters [63]. The scale parameters are basically the ratio of current density to magnetic field, and they show twisting or shearing of the magnetic field. The dimensions of these scale parameters are inverse of length, so the size of self-organized structures is determined by them whereas the behavior of relaxed state (paramagnetic or diamagnetic) depends on their nature (real or complex). The relation between these scale parameters and coefficients of QB equation (14) is $k_1 = \mu_1\mu_2\mu_3\mu_4$, $k_2 = \mu_1\mu_2\mu_3 + \mu_1\mu_2\mu_4 + \mu_1\mu_3\mu_4 + \mu_2\mu_3\mu_4$, $k_3 = \mu_1\mu_2 + \mu_2\mu_3 + \mu_1\mu_3 + \mu_1\mu_4 + \mu_2\mu_4 + \mu_3\mu_4$ and $k_4 = \mu_1 + \mu_2 + \mu_3 + \mu_4$. It is evident from above equations that the eigenvalues are roots of the following quartic equation

$$\mu^4 - k_4\mu^3 + k_3\mu^2 - k_2\mu + k_1 = 0. \quad (16)$$

It is critical to remember that plasma is considered to be incompressible in this study, all information about fields and flows in the relaxed state is contained within these scale parameters. The roots of above quartic equation (16) can be calculated using these relations

$$\mu_{1,2} = \frac{k_4}{4} + \frac{S \pm T}{2}, \quad (17)$$

$$\mu_{3,4} = \frac{k_4}{4} - \frac{S \pm L}{2}, \quad (18)$$

where $S = 0.5(k_4^2 - 4k_3 + 4R)^{1/2}$, $R = (\eta_3 k_3 + 3k_2 k_4 - 12k_1 - (3k_2^2 + 3k_1 k_4^2 - 12k_1 k_3 - k_3^2)^2 - k_3^2)\eta_3^{-1}$, $\eta_1 = (9k_2 k_3 k_4 - 36k_1 - 2k_3^3 - k_2^2 - 27k_1 k_4^2 + 108k_1 k_3)/54$, $\eta_2 = (3k_2 k_4 - 12k_1 - k_3^2)/9$ and $\eta_3 = 9((\eta_1^2 + \eta_2^3)^{1/2} + \eta_1)^{1/3}$. The T and L in case of $S \neq 0$ are given by $T = (0.75k_4^2 + 0.25S^{-1}(4k_3 k_4 - 8k_2 - k_4^2) - 2k_3 - S^2)^{1/2}$ and $L = (0.75k_4^2 - 0.25S^{-1}(4k_3 k_4 - 8k_2 - k_4^2) - 2k_3 - S^2)^{1/2}$ and in case of $S = 0$, $T = (2\sqrt{R^2 - 4k_1} + 0.75k_4^2 - 2k_3)^{1/2}$ and $L = (0.75k_4^2 - 2\sqrt{R^2 - 4k_1} - 2k_3)^{1/2}$.

From above relations it is clear that the scale parameters μ_j can be real or complex and their values depend on plasma parameters. Figure (1) shows the character of scale parameters of quartic equation ($f(\mu) = \mu^4 - k_4\mu^3 + k_3\mu^2 - k_2\mu + k_1$) for slightly, moderately and highly relativistic plasma species for given values of Beltrami parameters and density

($a = 2.0$, $b = 0.8$, $c = 3.0$, $G_i = 1.1$ and $N_i = 0.1$). In case of slightly relativistic plasma species i.e. $G = 1.2$, the two eigenvalues are real while other two are complex conjugate ($\mu_1 = 3.0$, $\mu_2 = 1.6709$ and $\mu_{3,4} = 0.5645 \pm 0.9889i$). By increasing the temperature to $G = 8.0$, all the scale parameters become real and given by $\mu_1 = 3.0$, $\mu_2 = 1.9386$, $\mu_3 = 0.5642$ and $\mu_4 = 0.291$. But in ultra-relativistic regime $G = 12.0$, again all the scale parameters are real ($\mu_1 = 3.0$, $\mu_2 = 1.9588$, $\mu_3 = 0.6780$ and $\mu_4 = 0.1631$). From plot it is also evident that with an increase in G the value of μ_4 reduces whereas μ_3 increases. It is important to highlight that such real scale parameters give rise to paramagnetic behavior in the relaxed state.

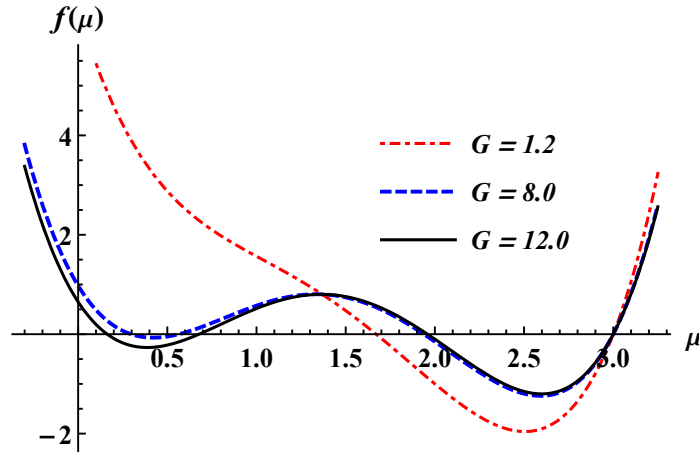


FIG. 1: Character of scale parameters for different values of relativistic temperatures when $a = 2.0$, $b = 0.8$, $c = 3.0$, $G_i = 1.1$ and $N_i = 0.1$.

Similarly figure (2) illustrates the character of scale parameters for fixed values of Beltrami parameters and thermal energies of plasma species ($a = 3.0$, $b = 1.5$, $c = 2.0$, $G = 1.5$ and $G_i = 1.1$) for various values of ion density ($N_i = 0.1, 0.6$ & 0.9). The plot demonstrates that for lower ion density, two eigenvalues are real and other two are complex. For instance when $N_i = 0.1$, the eigenvalues are $\mu_1 = 2.7954$, $\mu_2 = 1.9999$ and $\mu_{3,4} = 0.8523 \pm 0.5246i$. Whereas for higher concentrations scale parameters are real (when $N_i = 0.6$, the eigenvalues are real and given by $\mu_1 = 2.7767$, $\mu_2 = 1.9998$, $\mu_3 = 1.1683$ and $\mu_4 = 0.5550$, and in case of $N_i = 0.9$, the eigenvalues become $\mu_1 = 2.7633$, $\mu_2 = 1.9997$, $\mu_3 = 1.4338$ and $\mu_4 = 0.3031$). From the analysis of plot it is clear that by increasing ion density the scale separation between μ_3 and μ_4 increases. The occurrence of large and multiscale structures in hot astrophysical plasmas, as well as their interpretation, has been a long-standing challenge. Here, we'll look

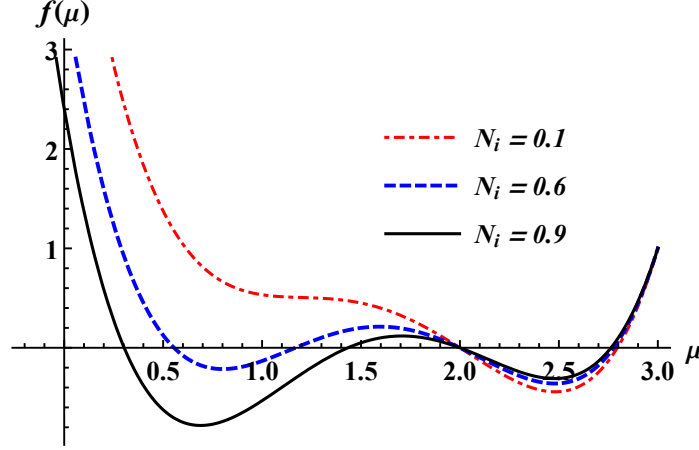


FIG. 2: Character of scale parameters for different values of N_i when $a = 3.0$, $b = 1.5$, $c = 2.0$ and $G = 1.5$ and $G_i = 1.1$.

at a few different possibilities to the design of system-size structures.

1. First we consider that $k_1 = 0$, then equation (16) can be written as $\mu(\mu^3 - k_4\mu^2 + k_3\mu - k_2) = 0$. The preceding equation demonstrates that at least one system size structure ($\mu_1 \sim 0$) exists in the relaxed state for this specific case. This is also quantitatively verifiable. For example, when $b = 1.7$, $c = 2.0$, $N_i = 0.1$, $G = 7.0$ and $G_i = 1.1$, the values of Beltrami parameter a and scale parameters are given by $a \approx -1.8883$, $|\mu_1| = 1.8 \times 10^{-17}$, $|\mu_2| = 1.809$, $|\mu_3| = 1.6227$ and $|\mu_4| = 2.0$. These scale parameters indicate that for $k_1 = 0$, $\mu_1 \approx 0$, $\mu_2 \approx a$, $\mu_3 \approx b$ and $\mu_4 \approx c$.
2. Consider an other possibility for the creation of two system size vortices i.e. $k_1 = k_2 = 0$. Then equation (16) can be written in the following form $\mu^2(\mu^2 - k_4\mu + k_3) = 0$, which leads to following values of scale parameters $\mu_{1,2} = 0$ and $\mu_{3,4} = 0.5(k_4 \pm \sqrt{k_4^2 - 4k_3})$. To confirm this fact we consider the following values of plasma parameters: $c = 2.0$, $N_i = 0.1$, $G = 7.0$ and $G_i = 1.1$, the values of Beltrami parameters (a, b) and the scale parameters are given by $a \approx -0.5492$, $b \approx 0.4943$, $|\mu_{1,2}| = 9.34 \times 10^{-9}$, $|\mu_3| = 2.0$ and $|\mu_4| = 0.05488$. These eigenvalues show that for $k_1 = k_2 = 0$, $\mu_{1,2} \approx 0$ and $\mu_3 \approx c$. This vast scale separation is important in the context of dynamo mechanisms in plasmas.
3. For three macro scale structures we consider $k_1 = k_2 = k_3 = 0$, then the quartic equation can be written as $\mu^3(\mu - k_4) = 0$, which yields the following eigenvalues: $\mu_{1,2,3} = 0$ and $\mu_4 = k_4$. For this case we consider $N_i = 0.1$, $G = 7.0$ and $G_i = 1.1$,

the values of Beltrami parameters (a , b , c) and the scale parameters are given by $a \approx 0.5536$, $b \approx -0.4967$, $c \approx 0.0621$, $|\mu_{1,2,3}| \approx 1.58 \times 10^{-6}$ and $|\mu_4| = 0.2$.

4. When the ratios of generalized vorticities to the flows for pair species are approximately equal i.e. $a \approx b$, the values of two scale parameters are $\mu_1 = a$ and $\mu_2 = c$.
5. When $a \approx b \approx c$, in this particular case two of roots are equal i.e. $\mu_1 \approx \mu_2 \approx a$.

IV. ANALYTICAL SOLUTION OF QB STATE

The magnetic fields and coupled flows in the QB state are controlled by four scale parameters. The size and nature of these scale parameters depends on Beltrami parameters, relativistic temperatures and density of the plasma species. To illustrate the effect of plasma parameters on the formation and nature of QB self-organized structures, we will use a simple slab geometry for an EPI plasma system. The general solution of QB equation (14) can be represented as the linear combination of four distinct Beltrami fields [63] and can be written as

$$\mathbf{B} = \sum_{j=1}^4 C_j \mathbf{B}_j, \quad (19)$$

where \mathbf{B}_j satisfies the following Beltrami condition $\nabla \times \mathbf{B}_j = \mu_j \mathbf{B}$. In a simple slab geometry, the magnetic field can be expressed as

$$\mathbf{B} = \sum_{j=1}^4 C_j [\sin(\mu_j x) \hat{y} + \cos(\mu_j x) \hat{z}], \quad (20)$$

where C_j are constants and their values are given in appendix A. The expression for composite flow velocity demands us to write its analytical solution in the following manner:

$$\mathbf{V} = \sum_{j=1}^4 F_j [\sin(\mu_j x) \hat{y} + \cos(\mu_j x) \hat{z}], \quad (21)$$

where $F_j = C_j (k_4 \mu_j^3 - k_3 \mu_j^2 + k_2 \mu_j - k_1)$. The existence After formulating the analytical solution for the QB magnetic field and associated flow, we may experiment with different arbitrary values of plasma parameters to determine how they affect relaxed state structures. For our current analysis of relaxed state structures, we consider pulsar magnetospheric plasma. At a distance of 10^8 cm from the pulsar surface, the electron density is $n_e = 10^6$ cm $^{-3}$ and the corresponding skin depth is 5.31×10^2 cm [27–29, 64].

A. Impact of relativistic temperature

Besides the Beltrami parameters, the thermal energy and density of plasma species have an important role in determining the magnitudes and nature of the scale parameters. As mentioned earlier, the impact of ion relativistic temperature is not significant due to large mass difference between pair and ion species. So, in order to investigate the effect of thermal energy of pair species, figure (3) shows the trend of magnetic field and flow when the values of Beltrami parameters, relativistic ion temperature and ion density are $a = 2.9$, $b = 1.3$, $c = 1.5$, $G_i = 1.1$ and $N_i = 0.1$, respectively. When the plasma species are slightly relativistic such that $G = 1.2$, the two eigenvalues are real ($\mu_1 = 1.5$, $\mu_2 = 2.6395$) and other two are complex conjugate ($\mu_{3,4} = 0.7802 \pm 0.7910i$). For these eigenvalues, the magnetic field shows diamagnetic behavior while bulk fluid velocity of plasma slightly decreases as strength of magnetic field increases. In the case of highly relativistic electrons and positrons i.e. $G = 7.0$, all the scale parameters are real and distinct and their values are $\mu_1 = 0.1656$, $\mu_2 = 1.1830$, $\mu_3 = 1.5$ and $\mu_4 = 2.8513$. These all real eigenvalues are consequence of higher thermal energies of pair species. Corresponding to real eigenvalues, the magnetic field structure shows paramagnetic behavior while flow has slightly increased as the magnetic field decreases. From figure (3), it is evident that for certain values of Beltrami parameters and ion density, an increase in thermal energies of plasma species transforms the diamagnetic structures into paramagnetic structures [5].

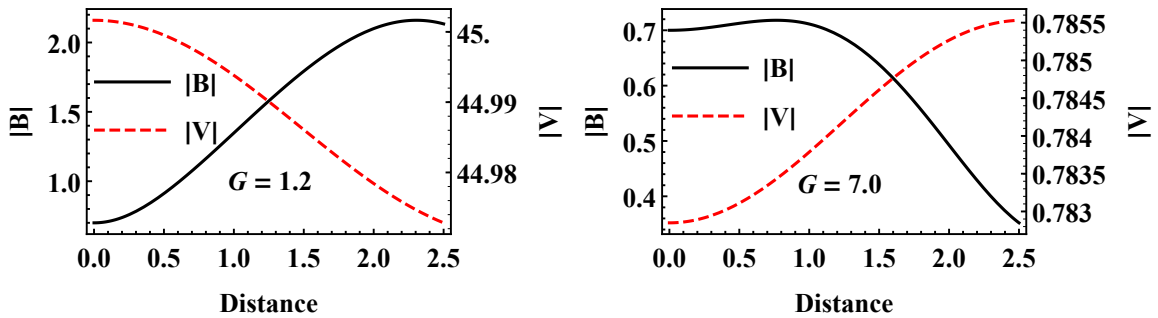


FIG. 3: Trend of magnetic field (left vertical axis) and flow (right vertical axis) for different values of relativistic temperature G (1.2 & 7.0) when $a = 2.9$, $b = 1.3$, $c = 1.5$, $G_i = 1.1$ and $N_i = 0.1$.

B. Impact of ion density

Figure (4) illustrates the effect of ion density on magnetic field and flow structures for given thermal energies and Beltrami parameters ($G = 7.0$, $G_i = 1.1$, $a = 1.1$, $b = 0.8$ and $c = 2.5$). For this set of plasma parameters when $N_i = 0.1$, two of eigenvalues are real while other two are complex and these are $\mu_1 = 2.4999$, $\mu_2 = 1.0118$ and $\mu_{3,4} = 0.4441 \pm 0.2356i$. For these eigenvalues, figure (4) shows diamagnetic behavior whereas flow trend is opposite to magnetic field. For higher ion density $N_i = 0.9$, the scale parameters are real and distinct, and have the following values: $\mu_1 = 2.4998$, $\mu_2 = 0.9641$, $\mu_3 = 0.7579$ and $\mu_4 = 0.1781$. For these real eigenvalues, Fig. (4) depicts that trend of magnetic field is paramagnetic and bulk fluid velocity also decreases. From above discussion, it can be concluded that for suitable Beltrami parameters, the ion species density and relativistic temperature have a key role in controlling the relaxed state structures. At higher relativistic temperatures and ion densities, the magnetic structures are paramagnetic while at lower values diamagnetic structures are formed.

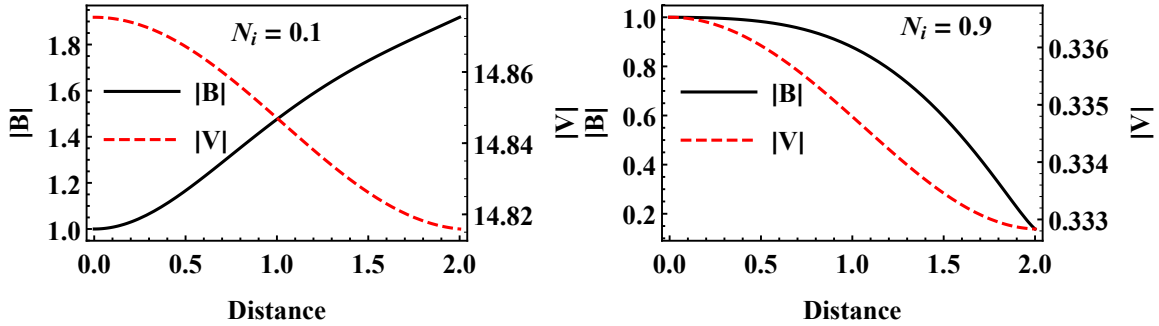


FIG. 4: Trend of magnetic field (left vertical axis) and flow (right vertical axis) for different values of ion density N_i (0.1 & 0.9) when $a = 1.1$, $b = 0.8$, $c = 2.5$, $G = 7.0$ and $G_i = 1.1$.

C. Role of scale separation on field and flow generation

The aforementioned study manifests a significant mutual coupling between the magnetic field and velocity in thermally relativistic EPI plasma. This interaction produces four self-organized structures corresponding to four scale parameters (μ_1 , μ_2 , μ_3 and μ_4). When the scale parameters are separated significantly, the magnetic field and the coupled velocity may have an appreciable difference. Now we investigate how disparate variations in the magnetic

field and velocity are influenced by the eigenvalues that are significantly disparate from one another (some of $|\mu_j| \gg 1$ and $|\mu_j| \ll 1$) in the context of dynamo mechanisms. The dynamo process is a fascinating subject in contemporary plasma physics, where magnetic fields are self-generated by a moving electrically conducting fluid. In this phenomenon, kinetic energy is transformed into magnetic energy [65, 66]. The reverse of this phenomenon, where magnetic energy is transformed to kinetic energy (generation of flow from a field), can also occur and is termed as reverse dynamo [21]. Although the dynamo and reverse dynamo mechanisms are time-dependent but these relaxed state fields and flows are the energy reservoir and provide the seeds for these mechanisms.

To see the glimpse of field and flow generation mechanisms in QB state, we consider two different regimes of Beltrami parameters while relativistic temperature of pair species and ion density values are varied. First, we assume that the values of Beltrami parameters are $a = 17.0$, $b = 16.0$ and $c = 15.0$ and relativistic temperature of ion species is $G_i = 1.1$. For this set of Beltrami parameters all the scale parameters are real and distinct. When ion density is high and pair species are mildly relativistic i.e., $N_i = 0.9$, $G = 1.2$ and $G_i = 1.1$, the eigenvalues are $\mu_1 \approx a$, $\mu_2 \approx b$, $\mu_3 \approx c$ and $\mu_4 = 0.05$. For these eigenvalues, figure (5-i) clearly demonstrates that the variation in the magnetic field is jittery, whereas the corresponding flow is smooth and strong. For highly relativistic plasma ($G = 7$) with small number of ions ($N_i = 0.1$), the scale parameters have the following values: $\mu_1 \approx a$, $\mu_2 \approx b$, $\mu_3 \approx c$ and $\mu_4 = 0.016$. Figure (5-ii) illustrates that the strength of the magnetic field and flow is drastically increased, despite the fact that the magnetic field continues to be jittery. The decrease in ion density as well as the increase in the effective masses of lighter species are the causes of this increase in flow and field. The plot depicts a smooth flow beside a fluctuating magnetic field.

Following the discussion presented above, it should be obvious that the flow is more powerful than the magnetic field ($V \gg B$) when the scale parameters reflect three microscale structures and one macroscale structure ($\mu_{1,2,3} \gg 1$ and $\mu_4 \ll 1$). From plots, one can also deduce that the small value of the magnetic field is being generated by the conversion of kinetic energy into magnetic energy. During this energy conversion process, the flow field is working against the Lorentz force [67]. So the presence of three microscales and one macroscale structure in QB state provide the seeds of a dynamo mechanism due to the dominance of kinetic energy over magnetic energy in the equilibrium state. The impact of

scale separation in the relaxed states on the time-dependent dynamo mechanism has been extensively investigated in recent years [20, 68, 69, 71].

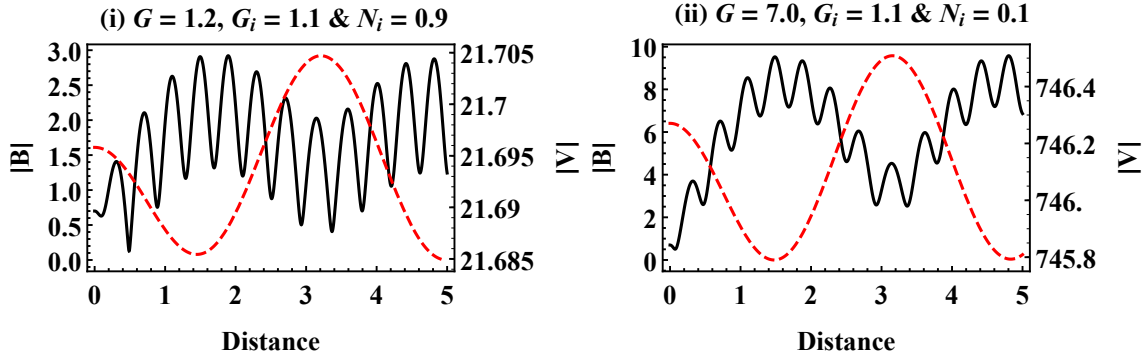


FIG. 5: Trend of magnetic field (jittery (solid) – left vertical axis) and flow (smooth (dashed) – right vertical axis) for different values of ion density and relativistic temperatures when $a = 17.0$, $b = 16.0$ and $c = 15.0$.

In the second case, we consider $a = 2.0$, $b = 4.0$, $c = 40.0$ and $G_i = 1.1$. For a slightly relativistic ($G = 1.2$) plasma with higher ion density ($N_i = 0.9$), the scale parameters are $\mu_1 = 0.6355$, $\mu_2 = 1.3834$, $\mu_3 \approx b$ and $\mu_4 \approx c$. Corresponding to these scale parameters, figure (6-i) demonstrates that the magnetic field is strong and smooth, but the flow is weak and jittery. In case of highly relativistic ($G = 7.0$) with a lower ion density ($N_i = 0.1$), the scale parameters have the following values: $\mu_1 = 0.10$, $\mu_2 \approx a$, $\mu_3 \approx b$ and $\mu_4 \approx c$. For this set of plasma parameters, figure (6-ii) shows that the strength of the field and flow is decreased, despite the flow continuing to be jittery. This decrease in field and flow is due to variation in scale separation caused by plasma parameters.

According to the description above and using equations (20-21) the relation between flow and field for these eigenvalues ($\mu_1 \ll 1$, $\mu_{2,3} \sim 1$ and $\mu_4 \gg 1$) shows that $V \ll B$ i.e., magnetic energy is dominant over kinetic energy. It is also very clear from figure (6) that variation in magnetic field is smooth but the accompanying flow is jittery and weak in comparison to the magnetic field. It seems that the Lorentz force is driving the plasma flow and thus converts the magnetic energy into kinetic energy. This conversion of magnetic energy into kinetic energy happens along with the viscous heating which is the consequence of positive work due to Lorentz force [70]. In a study pertaining to the heating of the solar corona, Mahajan et al. demonstrated that, due to scale separation in the relaxed state, the coupled magnetic field and flow can vary on vastly different length scales. So when a smooth

magnetic field is coupled with a jittery and weak flow, magnetic energy is dissipated along with the viscous heating of plasma [15]. So it is the scale separation in the relaxed state and the resulting jittery components in both vector fields that drive energy conversions via different scenarios. For this particular situation, we are able to draw the conclusion that the provision of the seeds for a reverse dynamo process is made possible when the magnetic energy in the equilibrium state is significantly larger than the kinetic energy. Such relaxed states where magnetic energy dominates the kinetic energy are also utilized to study time-dependent reverse dynamo processes [21, 71, 72]. The most recent study by Kotorashvili and Shatashvili investigated the unified dynamo and reverse dynamo mechanisms in a three-component plasma composed of static positive ions and two species of electrons: relativistic hot and relativistic degenerate [73]. So the mechanisms outlined here for the generation of fields and flows in a variety of astrophysical settings are extremely plausible.

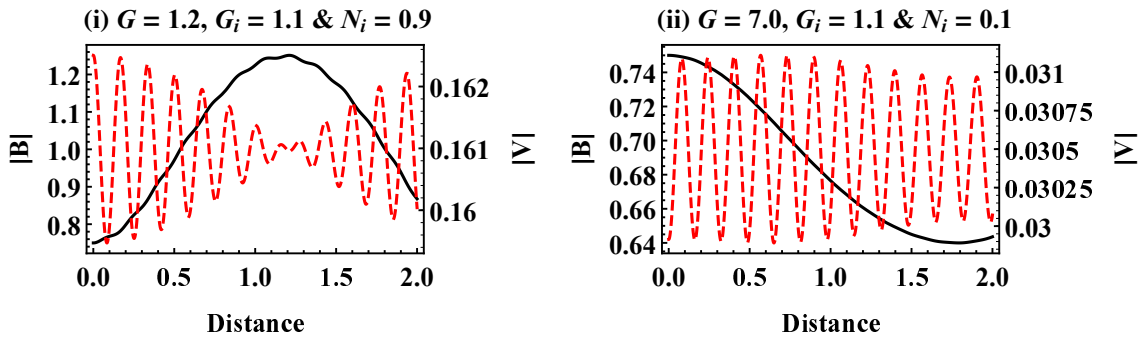


FIG. 6: Trend of magnetic field (smooth (solid) – left vertical axis) and flow (jittery (dashed) – right vertical axis) for different values of ion density and relativistic temperatures when $a = 2.0$, $b = 4.0$, and $c = 40.0$.

V. SUMMARY

The relaxation of a three-component thermally relativistic EPI magnetized plasma has been explored in this paper. It is assumed that all of the plasma species (electrons, positrons, and mobile positive ions) are relativistically hot and the relativistic temperatures of electrons and positrons are the same whereas the temperature of ion species is different in this model of EPI plasma. When the steady state solutions of the vorticity evolution equations for the

plasma species are coupled using Ampere's law, the relaxed state is a QB state, which is combination of four single and distinct Beltrami states. As a result, there are four scale parameters that describe the relaxed state of this plasma system. The analytical solution of the QB relaxed state in a simple slab geometry is provided in order to highlight the effect of plasma parameters on the magnetic field and flow structures. Following the study, it has been discovered that when the ion density and relativistic temperature of electron and positron species are higher for given values of Beltrami parameters, all the scale parameters are real and magnetic structures exhibit the paramagnetic trend. It is critical to emphasize that the influence of ion relativistic temperature is negligible on the relaxed state structures due to large mass difference between ion and pair species.

Additionally, it has been investigated that when three microscale structures along with a large scale structure are formed in QB state, the magnetic variation occurs at considerably shorter length scales as compared to flow. This flow and field pattern is an indicator that a magnetic field is being generated by the strong plasma flow. The field and flow trends are switched when there is a microscale structure, two structures of the order of electron skin depth and one large-scale structure. In the relaxed state, this flow field exhibits variations on shorter length scales which indicates the presence of turbulence. Such disparate variations in field and flow can provide the seeds for dynamo and reverse dynamo processes. These findings lead us to the conclusion that QB states are of great importance and can be used to better understand the creation of multiscale structures and related phenomena in thermally relativistic EPI plasmas found in astrophysical and laboratory plasmas.

Acknowledgments

The work of M. Iqbal is funded by Higher Education Commission (HEC), Pakistan under project No. 20-9408/Punjab/NRPU/R&D/HEC/2017-18. We are also thankful to the anonymous reviewer, whose insightful comments and suggestions helped us to improve the quality of the work.

Appendix A

The constants C_j can be calculated with the help of following boundary conditions: $|\mathbf{B}_z|_{x=0} = b_1$, $|\mathbf{B}_y|_{x=x_0} = b_2$, $|(\nabla \times \mathbf{B})_z|_{x=0} = b_3$ and $|(\nabla \times \mathbf{B})_y|_{x=x_0} = b_4$, where b_1 , b_2 , b_3 , b_4 and x_0 are arbitrary and real valued constants. The boundary conditions lead to these equations $\sum_{j=1}^4 C_j = b_1$, $\sum_{j=1}^4 C_j \sin(\mu_j x_0) = b_2$, $\sum_{j=1}^4 C_j \mu_j = b_3$ and $\sum_{j=1}^4 C_j \mu_j \sin(\mu_j x_0) = b_4$. By solving these boundary condition equations simultaneously one can obtain the values of C_j given by $C_j = K^{-1} R_j$ where

$$\begin{aligned} R_1 = & [(b_3 \mu_2 + b_1 \mu_3 \mu_4) \sin(\mu_2 x_0) - (b_4 \mu_2 + b_2 \mu_3 \mu_4)] [\sin(\mu_4 x_0) - \sin(\mu_3 x_0)] \\ & + [(b_3 \mu_3 + b_1 \mu_4 \mu_2) \sin(\mu_3 x_0) - (b_4 \mu_3 + b_2 \mu_4 \mu_2)] [\sin(\mu_2 x_0) - \sin(\mu_4 x_0)] \\ & + [(b_3 \mu_4 + b_1 \mu_3 \mu_2) \sin(\mu_4 x_0) - (b_4 \mu_4 + b_2 \mu_3 \mu_2)] [\sin(\mu_3 x_0) - \sin(\mu_2 x_0)], \end{aligned}$$

$$\begin{aligned} R_2 = & [(b_3 \mu_1 + b_1 \mu_3 \mu_4) \sin(\mu_1 x_0) - (b_4 \mu_1 + b_2 \mu_3 \mu_4)] [\sin(\mu_3 x_0) - \sin(\mu_4 x_0)] \\ & + [(b_3 \mu_3 + b_1 \mu_1 \mu_4) \sin(\mu_3 x_0) - (b_4 \mu_3 + b_2 \mu_1 \mu_4)] [\sin(\mu_4 x_0) - \sin(\mu_1 x_0)] \\ & + [(b_3 \mu_4 + b_1 \mu_1 \mu_3) \sin(\mu_4 x_0) - (b_4 \mu_4 + b_2 \mu_1 \mu_3)] [\sin(\mu_1 x_0) - \sin(\mu_3 x_0)], \end{aligned}$$

$$\begin{aligned} R_3 = & [(b_3 \mu_1 + b_1 \mu_2 \mu_4) \sin(\mu_1 x_0) - (b_4 \mu_1 + b_2 \mu_2 \mu_4)] [\sin(\mu_4 x_0) - \sin(\mu_2 x_0)] \\ & + [(b_3 \mu_2 + b_1 \mu_1 \mu_4) \sin(\mu_2 x_0) - (b_4 \mu_2 + b_2 \mu_1 \mu_4)] [\sin(\mu_1 x_0) - \sin(\mu_4 x_0)] \\ & + [(b_3 \mu_4 + b_1 \mu_1 \mu_2) \sin(\mu_4 x_0) - (b_4 \mu_4 + b_2 \mu_1 \mu_2)] [\sin(\mu_2 x_0) - \sin(\mu_1 x_0)], \end{aligned}$$

$$\begin{aligned} R_4 = & [(b_3 \mu_1 + b_1 \mu_2 \mu_3) \sin(\mu_1 x_0) - (b_4 \mu_1 + b_2 \mu_2 \mu_3)] [\sin(\mu_2 x_0) - \sin(\mu_3 x_0)] \\ & + [(b_3 \mu_2 + b_1 \mu_1 \mu_3) \sin(\mu_2 x_0) - (b_4 \mu_2 + b_2 \mu_1 \mu_3)] [\sin(\mu_3 x_0) - \sin(\mu_1 x_0)] \\ & + [(b_3 \mu_3 + b_1 \mu_1 \mu_2) \sin(\mu_3 x_0) - (b_4 \mu_3 + b_2 \mu_1 \mu_2)] [\sin(\mu_1 x_0) - \sin(\mu_2 x_0)], \end{aligned}$$

$$\begin{aligned} K = & (\mu_1 \mu_2 + \mu_3 \mu_4) [(\sin(\mu_1 x_0) - \sin(\mu_2 x_0)) (\sin(\mu_3 x_0) - \sin(\mu_4 x_0))] \\ & + (\mu_1 \mu_4 + \mu_3 \mu_2) [(\sin(\mu_1 x_0) - \sin(\mu_4 x_0)) (\sin(\mu_2 x_0) - \sin(\mu_3 x_0))] \\ & + (\mu_1 \mu_3 + \mu_4 \mu_2) [(\sin(\mu_2 x_0) - \sin(\mu_4 x_0)) (\sin(\mu_3 x_0) - \sin(\mu_1 x_0))]. \end{aligned}$$

In order to do a numerical analysis of the relaxed state, the following values of the boundary conditions are used (for Figs. 3 and 5): $b_1 = 0.7$, $b_2 = 0.25$, $b_3 = 0.2$ and $b_4 = 0.03$. Whereas,

for Fig. 4: $b_1 = 1.0$, $b_2 = 0.025$, $b_3 = 0.3$ and $b_4 = 0.5$, while for Fig. 6, these values are $b_1 = 0.75$, $b_2 = 0.35$, $b_3 = 0.2$ and $b_4 = 0.03$.

-
- [1] Woltjer L 1958 Proc. Natl. Acad. Sci. 44 489–91
 - [2] Taylor J B 1974 Phys. Rev. Lett. 33 1139–41
 - [3] Taylor J B 1986 Rev. Mod. Phys. 58 741–63
 - [4] Steinhauer L C and Ishida A 1997 Phys. Rev. Lett. 79 3423–6
 - [5] Mahajan S M and Yoshida Z 1998 Phys. Rev. Lett. 81 4863–6
 - [6] Steinhauer L C 2002 Phys. Plasmas 9 3767–74
 - [7] Bhattacharyya R, Janaki M S and Dasgupta B 2003 Phys. Lett. A 315 120–5
 - [8] Iqbal M 2013 Appl. Phys. Lett. 103 034109
 - [9] Iqbal M and Shukla P K 2012 Phys. Plasmas 19 033517
 - [10] Mahajan S M and Lingam M 2015 Phys. Plasmas 22 092123
 - [11] Ullah S, Shazad U and Iqbal M 2022 Phys. Scr. 97 65605
 - [12] Mahajan S M and Yoshida Z 2000 Phys. Plasmas 7 635–40
 - [13] Yoshida Z, Mahajan S M, Ohsaki S, Iqbal M and Shatashvili N 2001 Phys. Plasmas 8 2125–31
 - [14] Guzdar P N, Mahajan S M and Yoshida Z 2005 Phys. Plasmas 12 032502
 - [15] Mahajan S M, Miklaszewski R, Nikol’skaya K I and Shatashvili N L 2001 Phys. Plasmas 8 1340–57
 - [16] Mahajan S M, Nikol’skaya K I, Shatashvili N L and Yoshida Z 2002 Astrophys. J. 576 L161–4
 - [17] Ohsaki S, Shatashvili N L, Yoshida Z and Mahajan S M 2002 Astrophys. J. 570 395–407
 - [18] Kagan D and Mahajan S M 2010 Mon. Not. R. Astron. Soc. 406 1140–5
 - [19] Mahajan S M, Shatashvili N L, Mikeladze S V and Sigua K I 2006 Phys. Plasmas 13 062902
 - [20] Mininni P D, Gómez D O and Mahajan S M 2002 Astrophys. J. 567 L81–3
 - [21] Mahajan S M, Shatashvili N L, Mikeladze S V. and Sigua K I 2005 Astrophys. J. 634 419–25
 - [22] Abdelhamid H M, Lingam M and Mahajan S M 2016 Astrophys. J. 829 87
 - [23] Mahajan S M and Lingam M 2020 Mon. Not. R. Astron. Soc. 495 2771–6
 - [24] Holcomb K A and Tajima T 1989 Phys. Rev. D 40 3809–18
 - [25] Sturrock P A 1971 Astrophys. J. 164 529–56
 - [26] Ruderman M A and Sutherland P G 1975 Astrophys. J. 196 51–72

- [27] Karpman V I, Norman C A, Ter Haar D and Tsytovich V N 1975 Phys. Scr. 11 271–4
- [28] Melrose D B 1978 Astrophys. J. 225 557–73
- [29] Michel F C 1982 Rev. Mod. Phys. 54 1–66
- [30] Liang E P and Dermer C D 1988 Astrophys. J. 325 L39–42
- [31] Begelman M C, Roger D B and Rees M J 1984 Rev. Mod. Phys. 56 255–351
- [32] Furlanetto S R and Loeb A 2002 Astrophys. J. 569 L91–4
- [33] Martin P, Vink J, Jiraskova S, Jean P and Diehl R 2010 Astron. Astrophys. 519 A100
- [34] Murphy R J, Share G H, Skibo J G and Kozlovsky B 2005 Astrophys. J. Suppl. Ser. 161 495–519
- [35] Surko C M et al. 1986 Rev. Sci. Instrum. 57 1862–7
- [36] Greaves R G and Surko C M 1997 Phys. Plasmas 4 1528–43
- [37] Helander P and Ward D J 2003 Phys. Rev. Lett. 90 135004
- [38] Fajans J and Surko C M 2020 Phys. Plasmas 27 030601
- [39] Sarri G et al. 2015 Nat. Commun. 6 6747
- [40] Peebles J L et al. 2021 Phys. Plasmas 28 074501
- [41] Iqbal M, Berezhiani V I and Yoshida Z 2008 Phys. Plasmas 15 032905
- [42] Iqbal M and Shukla P K 2012 J. Plasma Phys. 78 207–10
- [43] Iqbal M and Shukla P K 2013 J. Plasma Phys. 79 1–6
- [44] Pino J, Li H and Mahajan S 2010 Phys. Plasmas 17 112112
- [45] Shazad U, Iqbal M and Ullah S 2021 Phys. Scr. 96 125627
- [46] Berezhiani V I, Shatashvili N L and Mahajan S M 2015 Phys. Plasmas 22 022902
- [47] Shatashvili N L, Mahajan S M and Berezhiani V I 2016 Astrophys. Space Sci. 361 70
- [48] Shatashvili N L, Mahajan S M and Berezhiani V I 2019 Astrophys. Space Sci. 364 148
- [49] Bhattacharjee C, Das R, Stark D J and Mahajan S M 2015 Phys. Rev. E 92 063104
- [50] Bhattacharjee C, Feng J C and Mahajan S M 2019 Phys. Rev. D 99 24027
- [51] Asenjo F A and Mahajan S M 2019 Phys. Rev. E 99 53204
- [52] Bhattacharjee C 2020 Phys. Lett. A 384 126698
- [53] Pokhotelov O A, Onishchenko O G, Pavlenko V P, Stenflo L, Shukla P K, Bogdanov A V. and Kamenets F F 2001 Astrophys. Space Sci. 277 497-505
- [54] Eliasson B and Shukla P K 2005 Phys. Plasmas 12 1-4
- [55] Tsintsadze N L, Chaudhary R and Rasheed A 2013 J. Plasma Phys. 79 587-96

- [56] Rozina C, Tsintsadze N L, Jamil M, Rasheed A and Ali S 2014 *Astrophys. Space Sci.* 353 485-91
- [57] Lu D, Li Z L and Xie B S 2015 *J. Plasma Phys.* 81 905810508
- [58] Petropoulou M, Sironi L, Spitkovsky A and Giannios D 2019 *Astrophys. J.* 880 37
- [59] Zhdankin V, Uzdensky D A, Werner G R and Begelman M C 2019 *Phys. Rev. Lett.* 122 55101
- [60] Zhdankin V, Uzdensky D A and Kunz M W 2021 *Astrophys. J.* 908 71
- [61] Berezhiani V I and Mahajan S M 1995 *Phys. Rev. E* 52 1968–79
- [62] Mahajan S M 2008 *Phys. Rev. Lett.* 100 075001
- [63] Yoshida Z and Giga Y 1990 *Math. Zeitschrift* 204 235–245
- [64] Lazarus I J, Bharuthram R, Singh S V., Pillay S R and Lakhina G S 2012 *J. Plasma Phys.* 78 621
- [65] Vainshtein S I and Zeladovich Y B 1972 *Sov. Phys. Usp.* 15 159
- [66] Moffatt H K 1978 *Magnetic Field Generation in Electrically Conducting Fluids*, p.353 Cambridge University Press.
- [67] Moffatt H K and Proctor M R E 1985 *J. Fluid Mech.* 154 493
- [68] Mininni P D, Gomez D O and Mahajan S M 2003 *Astrophys. J.* 584 1120
- [69] Mahajan S M, Mininni P D and Gomez D O 2005 *Astrophys. J.* 619 1014
- [70] Brandenburg A and Rempel M 2019 *Astrophys. J.* 879 57
- [71] Lingam M and Mahajan S M 2015 *Mon. Not. R. Astron. Soc. Lett.* 449 L36
- [72] Kotorashvili K, Revazashvili N and Shatashvili N L 2020 *Astrophys. Space Sci.* 365 175
- [73] Kotorashvili K and Shatashvili N L 2022 *Astrophys. Space Sci.* 367 2